ACS OMEGA

Open Access

This article is licensed under CC-BY-NC-ND 4.0

http://pubs.acs.org/journal/acsodf

Article

Formally Exact and Practically Useful Analytic Solution of Harmonium

Wenqing Yao, Zhiyuan Yin, and Chen Li*

Cite This: *ACS Omega* 2024, 9, 46138−46147

Read Online

ACCESS | Metrics & More | Article Recommendations

ABSTRACT: We provide a novel exact analytic solution of harmonium with arbitrary Coulomb interaction strength, for ground as well as all the excited states, using our recently developed method for solving Schrödinger equations. By comparing three formally exact analytic representations of the wave function including the one that utilizes biconfluent Heun function, we find that the best and practically useful representation for the ground state is given by an exact factorized form involving a noninteger power pre-exponential factor, an exponentially decaying term and a modulator function. For excited states, additional factors are needed to account for the nodal information. We show that our method is far more efficient than basis-expansion-based methods in representing the wave function. With the exact wave functions, we have also analyzed the evolution trends of the electron density and natural occupation numbers with increasing interaction strength, which gives insight into the interesting physics in the strong correlation limit.

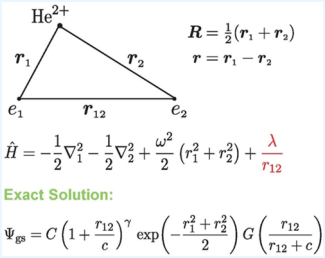

1. INTRODUCTION

Many-electron Schrödinger equations (SEs) are usually regarded as too complicated to have exact analytic solutions expressible in closed forms. The major difficulty is attributed to the presence of the electron−electron interaction. The quest for the exact solution of the simplest real-world two-electron problem, the helium atom, dates back to the early ages of quantum mechanics until the present day.[1−7] In 1962, Kestner and Sinanoğlu proposed a modified version of the helium atom by replacing the one-body nuclear Coulomb attraction terms by harmonic potentials while keeping the true two-electron Coulomb interaction.[8] This model system has several different names such as harmonic helium, (two-electron) Hooke's atom or harmonium. The Hamiltonian for harmonium in atomic units is

$$\hat{H} = -\frac{1}{2}(\nabla_1^2 + \nabla_2^2) + \frac{1}{2}\omega^2(r_1^2 + r_2^2) + \frac{\lambda}{r_{12}} \quad (1)$$

Here r_1 and r_2 are the distance between the nucleus and the two electrons, respectively, and $r_{12} = |\boldsymbol{r}_1 - \boldsymbol{r}_2|$ is the distance between the electrons. ω and λ are parameters that tune the interaction strengths of the potentials.

Although the real Coulomb physics of helium atom is partially lost in harmonium, one can take advantage of the modified potentials to study the electron correlation more easily. Applications of such models can be found, for example, in the simulation of quantum dots.[9−13] In particular, the special feature of harmonic one-body potentials allows one to separate variables, as was first utilized in ref 8. to simplify the numerical calculation of the correlation energy. Even more interestingly, it was found decades later that for specific ratios $\frac{\lambda^2}{\omega}$, the harmonium problem has simple exact analytic solutions, which could be ground or excited states;[14,15] and Taut proposed a method to systematically find these special solutions along with the corresponding parameter ratios.[15] For general $\frac{\lambda^2}{\omega}$ ratios, however, such simple solutions were not found. Although Karwowski and Witek have found that the exact solution of harmonium can be expressed formally in terms of biconfluent Heun function, a special function that has an infinite series expression,[16] this special function critically depends on the unknown energy, and we will show that this representation is not a practically useful one. In addition to the search for exact formulas, numerical solutions were obtained through various approximations including perturbation approaches, variational methods and wave function expansions.[17−20] Besides applications in wave function theory,[21] these solutions have been useful for studying the exchange-correlation hole in density functional theory,[22] and benchmarking the performance of various density functional approximations (DFAs),[23−27] including the very recent work of studying the violation of exact conditions of DFAs particularly when the ratio $\frac{\lambda^2}{\omega}$ varies.[28]

It would be desirable to generalize the exact analytic solutions of harmonium to arbitrary parameters. On the one

Received: July 19, 2024
Revised: October 12, 2024
Accepted: October 29, 2024
Published: November 8, 2024

© 2024 The Authors. Published by American Chemical Society

hand, this shall greatly enhance our understanding of the analytic structure of two-body wave functions, particularly in the case of Coulombic two-electron potential, for which we have very limited knowledge and very rare examples of such exact solutions. On the other hand, the existence of special solutions imply that this generalization is plausible; and we have a chance to use a unified analytic formula to encompass the exact solution for all parameters. In the quest of such unified formula, we can also uncover the mystery of the special ratios.

Recently, we have developed a novel method to solve the SEs and demonstrated through several examples that there exists simple and elegant forms of the stationary wave functions for a general one-electron SE. These examples include the one-dimensional (1D) hydrogen atom[29,30] and hydrogen molecular ion H_2^+ with soft Coulomb potential,[30,31] and the real-world 3D H_2^+.[32] In contrast to the conventional methods, our new method reformulates the ground state wave function as $\psi = Ce^{\beta}$, and transforms the SE, which is a second-order linear differential equation with respect to ψ, into the Riccati equation,[33] which is a first-order nonlinear differential equation with respect to the derivative of β. Then we perform particular variable transformations and Taylor expansions to this derivative subsequently, which lead to algebraic equations for the expansion coefficients. The resulting formula for the wave functions have unified analytic structures, including a power prefactor, an exponential decay and a modulator function on the exponent which is bounded and has a series expression. The formula for the excited states can be deduced similarly once we factorize the nodal factors from e^{β}. Although these formulas are not in closed forms, in the sense that they involve infinite series that cannot be truncated, they are useful analytic formulas because each of the series coefficients is known as an explicit function of the eigenstate energy, and the energy can be very efficiently obtained by solving an algebraic equation, as will be revisited later in the method section.

In this paper, we extend our new method from one-electron problems to the simplest two-electron problem, the harmonium. In particular, we extend the exact analytic solution from specific $\frac{\lambda^2}{\omega}$ ratios to arbitrary parameters for ground as wells as excited states. As found in our previous work, here we reiterate that our method has computational advantage over the basis expansion method.

2. METHODS

First of all, for two-electron eigenstate problems, the full wave function can be written as a product of a spatial wave function Ψ and a spin wave function Φ. The antisymmetry requirement of the full wave function demands that Ψ and Φ have opposite permutation symmetry. In particular, for singlet states Φ is antisymmetric and Ψ is symmetric, while for triplet states it is the other way round. Then it suffices to discuss only the spatial wave function Ψ. As will be shown, permutation symmetry is naturally built in the eigenstate solutions of $\hat{H}$, meaning that they are always simultaneously eigenstates of the permutation operator and thus correspond to legitimate solutions once paired with proper spin wave functions.

Second, we note that eq 1 which parametrically depends on ω and λ can be transformed into the problem where $\omega = 1$. In particular, one can show that the spatial wave function satisfies the following scaling relation: $\Psi(\boldsymbol{r}_1, \boldsymbol{r}_2; \omega, \lambda) = \omega^{3/2}\Psi\left(\sqrt{\omega}\boldsymbol{r}_1, \sqrt{\omega}\boldsymbol{r}_2; 1, \frac{\lambda}{\sqrt{\omega}}\right)$. Therefore, we will set $\omega = 1$ in the following discussions without loss of generality. For harmonic one-body potentials, it has been known that one can separate variables in the centroid coordinate.[8] Let $\boldsymbol{R} = \frac{1}{2}(\boldsymbol{r}_1 + \boldsymbol{r}_2)$ and $\boldsymbol{r} = \boldsymbol{r}_1 - \boldsymbol{r}_2$, the total spatial wave function can be rewritten as $\Psi(\boldsymbol{r}_1, \boldsymbol{r}_2) = \chi(\boldsymbol{R})\psi(\boldsymbol{r})$, where χ and ψ satisfy the following SEs, respectively:

$$\left(-\frac{1}{4}\nabla_{\boldsymbol{R}}^2 + R^2\right)\chi(\boldsymbol{R}) = E_R\chi(\boldsymbol{R}) \tag{2}$$

$$\left(-\nabla_{\boldsymbol{r}}^2 + \frac{r^2}{4} + \frac{\lambda}{r}\right)\psi(r) = E_r\psi(r) \tag{3}$$

The total energy is given by $E = E_R + E_r$. eq 2 is a 3D isotropic harmonic oscillator problem, whose solution in spherical coordinates depends on three quantum numbers (nlm),

$$\chi_{nlm}(\boldsymbol{R}) = CR^l L_n^{l+1/2}(2R^2)e^{-R^2}Y_l^m(\hat{\boldsymbol{R}}) \tag{4}$$

Here $C = \left(\frac{8}{\pi}\right)^{1/4}\sqrt{\frac{2^{n+2l+2}n!}{(2n+2l+1)!!}}$ is the normalization constant; $L_n^{l+1/2}$ is the generalized Laguerre polynomial; and Y_l^m is the spherical harmonic function that depends on the angular coordinates, denoted using the radial unit vector $\hat{\boldsymbol{R}}$ for brevity.

Equation 3 differs from a harmonic problem by the Coulombic term $\frac{\lambda}{r}$. But because the potential has spherical symmetry, one can again separate the angular part from the radial function, i.e., $\psi_{nlm}(\boldsymbol{r}) = \phi_{nl}(r)\ Y_l^m(\hat{\boldsymbol{r}})$, and the problem reduces to solving the following SE for the radial function ϕ_{nl}:

$$\left[-\frac{d^2}{dr^2} - \frac{2}{r}\frac{d}{dr} + \frac{r^2}{4} + \frac{\lambda}{r} + \frac{l(l+1)}{r^2}\right]\phi_{nl}(r) = E_r\phi_{nl}(r) \tag{5}$$

For some particular λ, eq 5 has a closed-form solution. For example, the ground state solution for $\lambda = \sqrt{2}$ is given by $\phi_{00}(r) = C_0\left(1 + \frac{r}{\sqrt{2}}\right)e^{-r^2/4}$, with $C_0 = \sqrt{\frac{2\sqrt{2}}{8+5\sqrt{\pi}}}$ and $E_r = \frac{5}{2}$.[15] For arbitrary λ, however, such an analytic solution remains unknown and is the key problem to be addressed in this paper.

We start by considering the ground state problem where $l = 0$. Because the wave function is nodeless on its domain $[0, \infty)$,[34] we can reformulate it in an exponential form: $\phi_{00}(r) = Ce^{\beta(r)}$. One can deduce the equation for β as the following:

$$-\frac{d^2\beta}{dr^2} - \left(\frac{d\beta}{dr}\right)^2 - \frac{2}{r}\frac{d\beta}{dr} + \frac{r^2}{4} + \frac{\lambda}{r} = E_r \tag{6}$$

Equation 6 is a first-order ordinary differential equation (ODE) of $v(r) \equiv \frac{d\beta}{dr}$. It is preferable to transform r onto a finite interval $[0,1)$. Here we invoke a fractional linear transformation $z = \frac{r}{r+c}$, where $c > 0$ is a constant. Following our idea in ref 31, the next step is to expand v as a function of z into Taylor series. However, because of the presence of the harmonic term $\frac{r^2}{4}$ in the potential, one can show that $v(z)$ has a first-order pole at $z = 1$. To remove this pole, we introduce $u(z) = (1 - z)v(z)$ and the resulting ODE for $u(z)$ reads

$$P_1(z)\frac{du}{dz} + P_2(z)u^2 + P_3(z)u + P_4(z) = 0 \tag{7}$$

https://doi.org/10.1021/acsomega.4c06679
ACS Omega 2024, 9, 46138−46147

where $P_1(z) = -z(1-z)^3$, $P_2(z) = -c$, $P_3(z) = -(1+2z)(1-z)^2$ and $P_4(z) = \frac{1}{4}c^3z^4 + \lambda z(1-z)^3 - E_r cz^2(1-z)^2$. Equation 7 is a Riccati equation that depends on E_r as a parameter, which is completely equivalent to the Schrödinger eq 5 for the ground state. The fact that the ground state energy has to take specific value is because the wave function decays to zero at $r \to \infty$, and one can show that this boundary condition of SE translates to the condition that u is finite and has finite derivative at $z = 1$. To solve for u, we expand it into the following Taylor series,

$$u(z) = \sum_{k=0}^{\infty} u_k z^k \tag{8}$$

where $u_0 \neq 0$. Here we assume that the radius of convergence can reach 1 and numerical results show that this assumption is valid. Plugging eq 8 into eq 7 and comparing terms order by order, we can derive recursive relations for u_k as follows,

$$u_k = -\frac{1}{kP_1^1 + 2P_2^0 u_0 + P_3^0}\left[\sum_{l=2}^{k}(k-l+1)P_1^l u_{k-l+1} - c\sum_{l=1}^{k-1} u_l u_{k-l} + \sum_{l=1}^{k} P_3^l u_{k-l} + P_4^k\right] \tag{9}$$

Here P_i^j is the jth-order Taylor coefficient of $P_i(z)$. Moreover, substituting $z = 0$ and $z = 1$ into eq 7, we obtain another two algebraic equations for u_k's:

$$P_2(0)u_0^2 + P_3(0)u_0 = 0 \tag{10}$$

$$P_2(1)\left(\sum_{k=0}^{\infty} u_k\right)^2 + P_4(1) = 0 \tag{11}$$

From eq 10 we deduce $u_0 = -\frac{P_3(0)}{P_2(0)}$. Then plugging u_0 and u_k into eq 11, we arrive at a series equation that depends on E_r. In practical calculations, we truncate the infinite series to N terms, leading to a polynomial equation of E_r, which can be solved iteratively using Newton's method. It is clear that enlarging N shall lead to increasingly accurate energy; as we will see later, energy convergence with N is extremely fast.

Next, we derive the formula for β. By the chain rule,

$$\frac{d\beta}{dr} = \frac{(1-z)^2}{c}\frac{d\beta}{dz} = \frac{1}{1-z}\sum_{k=0}^{\infty} u_k z^k \tag{12}$$

Therefore, $\beta(z)$ can be obtained by integration,

$$\beta(z) = c\sum_{k=0}^{\infty} u_k \int^z \frac{t^k}{(1-t)^3}dt = -\frac{\alpha}{(1-z)^2} + \frac{\eta}{1-z} - \gamma\ln(1-z) + F(z) \tag{13}$$

where $\alpha = -\frac{c}{2}\sum_{k=0}^{\infty} u_k = -\frac{c}{2}u(1)$, $\eta = -c\sum_{k=0}^{\infty} k u_k = -cu^{(1)}(1)$, $\gamma = \frac{c}{2}\sum_{k=0}^{\infty} k(k-1)u_k = \frac{c}{2}u^{(2)}(1)$ and $F(z) = \sum_{m=1}^{\infty} u^{(m+2)}(1)\frac{(-1)^{(m+1)}}{m(m+2)!}(1-z)^m$. Here $u^{(k)}(1)$ denotes the kth derivative of $u(z)$ evaluated at $z = 1$. Using the boundary condition ($z = 1$) of eq 7 and its derivatives, we can deduce $\alpha = \frac{1}{4}$, $\eta = \frac{1}{2}$ and $\gamma = E_r - \frac{3}{2}$. Of particular interest is the function $F(z)$, which we refer to as the modulator that also appeared in the exact solution of other SEs.[31] In spite of an infinite series, it is a bounded function that varies mildly on $[0, 1]$. Finally, rewritten in terms of r, the ground state wave function simplifies to

$$\phi_{00}(r) = C\left(1 + \frac{r}{c}\right)^{\gamma}\exp\left[-\frac{r^2}{4} + F\left(\frac{r}{r+c}\right)\right] \tag{14}$$

It is governed by a Gaussian decay, with a pre-exponential factor being a power function of $1 + \frac{r}{c}$ and a modulator on the exponent. This structure is consistent with the special solution when $\lambda = \sqrt{2}$, for which γ reduces to an integer 1 and the modulator F reduces to constant zero upon choosing $c = \sqrt{2}$. As an additional remark, although the wave function expression (14) formally depends on c that can be chosen arbitrarily, this arbitrariness is exactly canceled out by the c-dependent pre-exponential term and the modulator, making ϕ_{00} independent of c in reality.

The above procedures can be modified to target excited states. In particular, to account for the nodal positions $\{r_i\}_{i=1}^n$, we formulate excited state wave functions as $\phi_{nl}(r) = C\prod_{i=1}^n(r - r_i)\, e^{\beta(r)}$ and rewrite the SE (5) into a Riccati equation for $v = \frac{d\beta}{dr}$. Again we make variable transformation $z = \frac{r}{r+c}$ and denote $z_i = \frac{r_i}{r_i + c}$. Differing from the case where $l = 0$, the presence of $\frac{l(l+1)}{r^2}$ in the potential leads to an additional first-order pole of $v(z)$ at $z = 0$. Therefore, we introduce $w(z) = z(1-z)v(z)$ to eliminate all the poles, and the resulting Riccati equation resembles eq 7:

$$Q_1(z)\frac{dw}{dz} + Q_2(z)w^2 + Q_3(z)w(z) + Q_4(z) = 0 \tag{15}$$

Here $Q_1(z) = -cz(1-z)^3S(z)$, $Q_2(z) = -c^2S(z)$, $Q_3(z) = -c(1+2z)(1-z)^2S(z) - 2cz(1-z)^2S'(z)$ and $Q_4(z) = \left[\frac{1}{4}c^4z^4 + \lambda cz(1-z)^3 + l(l+1)(1-z)^4 - E_r c^2 z^2(1-z)^2\right]S(z) - 2z(1-z)^4S'(z) - 2z^2(1-z)^4S''(z)$, where $S(z) = \prod_{i=1}^n(z - z_i)$ contains the nodal information.

Expanding $w(z)$ into a Taylor series and plugging into eq 15, we can derive recursive relations for the Taylor coefficients w_k. The boundary conditions at $z = 0$ and $z = 1$ lead to analogous equations as eqs 10 and 11. Nevertheless, these are insufficient to determine E_r and w_k's because now we have additional n nodes as unknown variables. The additional conditions can be obtained by substituting z_i's into eq 15, which lead to algebraic equations given that $Q_1(z_i) = 0$. One can then solve for E_r, $\{w_k\}$ and $\{z_i\}$ together using multidimensional Newton's iteration method. Then repeating the steps as in solving for the ground state, we can obtain the formula for the excited wave functions:

$$\phi_{nl}(r) = Cr^l\left(1 + \frac{r}{c}\right)^{\gamma'}\prod_{i=1}^n(r - r_i)\exp\left[-\frac{r^2}{4} + F\left(\frac{r}{r+c}\right)\right] \tag{16}$$

Here, $\gamma' = E_r - n - l - \frac{3}{2}$, and one has to replace u by w in the definition of modulator F. eq 16 is similar to eq 14, but has additional factors of r^l and $\prod_{i=1}^n(r - r_i)$. This form suggests that the asymptotic behavior of $\phi_{nl} \sim r^{E_r - 3/2}e^{-r^2/4}$. Inspired by

https://doi.org/10.1021/acsomega.4c06679
ACS Omega 2024, 9, 46138−46147

this analytic structure, here we propose another equivalent formula by bringing the modulator down the exponent,

$$\phi_{nl}(r) = Cr^l\left(1 + \frac{r}{c}\right)^{\gamma} e^{-r^2/4} G\left(\frac{r}{r+c}\right) \tag{17}$$

Here $\gamma = \gamma' + n = E_r - l - 3/2$; and the relation between G and F is given by

$$G\left(\frac{r}{r+c}\right) = \left(1 + \frac{r}{c}\right)^{-n} \prod_{i=1}^{n} (r - r_i) e^{F\left(\frac{r}{r+c}\right)} \tag{18}$$

One can verify that $G(z)$ does not have poles in the unit circle so that it can be expanded into Taylor series, $G(z) = \sum_{k=0}^{\infty} G_k z^k$. In fact, it is as nicely behaved (bounded and slowly varying) as function $F(z)$; and for this reason we decide to refer to both functions as modulator rather than give another name for $G(z)$.

For practical computations, it turns out that formulating equation in terms of G saves more computational effort. In particular, G satisfies a second-order ODE:

$$p_1(z)\frac{d^2G}{dz^2} + p_2(z)\frac{dG}{dz} + p_3(z)G(z) = 0 \tag{19}$$

where $p_1(z) = z(1 - z)^3$, $p_2(z) = (2\gamma - 2)z(1 - z)^2 + (2l + 2)(1 - z)^2 - c^2z^2$ and $p_3(z) = c^2\gamma z - c\lambda + \gamma(\gamma + 2l + 1)z(1 - z) + 2\gamma(l + 1)(1 - z)^2$. eq 19 is linear in G, which is in contrast to the Riccati eqs 7 and 15 that are nonlinear. By expanding G in Taylor series and comparing terms in eq 19, the Taylor coefficients G_k has the following recursive relation:

$$G_{k+1} = -\frac{1}{(k+1)(2l+2+k)}\left[\sum_{i=2}^{k} p_1^i(k - i + 2)(k - i + 1) G_{k-i+2} + \sum_{i=1}^{k} p_2^i(k - i + 1)G_{k-i+1} + \sum_{i=0}^{k} p_3^i G_{k-i}\right] \tag{20}$$

Here p_i^j is the jth-order Taylor coefficient of $p_i(z)$. One can readily solve γ and E_r using the recursive relation (20) along with the boundary conditions of eq 19 at $z = 0$ and $z = 1$.

The computational advantages of (eq 19) over eq 15 are as follows. First, the linearity in G induces much simpler recursive relations of G_k than those for u_k or w_k. Second, (19) is applicable to both the ground and excited states so that the computational complexity does not grow with increasing nodes. Moreover, these merits are not at the cost of more terms in the expansion; in fact the formulation using F or G need similar number of expansion coefficients to represent a wave function at a given accuracy. For the above reasons, we recommend eq 17 as the best representation of the wave function. It follows that the total ground state wave function of harmonium can be written as

$$\begin{aligned}\Psi_0(\mathbf{r}_1, \mathbf{r}_2) &= \zeta_0(\mathbf{R}) \times \psi_0(\mathbf{r}) \\ &= C\left(1 + \frac{r}{c}\right)^{\gamma} e^{-(r_1^2 + r_2^2)/2} G\left(\frac{r}{r+c}\right)\end{aligned} \tag{21}$$

Here we have recast the wave function in terms of the distances between electrons and the nucleus. The ground state wave function is invariant to the collective rotation of particles, which is also true for the real-world helium atom with Coulombic nuclear attraction.[2] The formula for the excited states has additional factors on the basis of eq 21, including r^l, $Y_l^m(\hat{\mathbf{r}})$ and additional factors involving $\mathbf{R}$ that appears in eq 4. One can readily verify that the permutation symmetry of $\Psi(\mathbf{r}_1, \mathbf{r}_2)$ is governed by l: it is symmetric when l is even and leads to a singlet state; it is antisymmetric when l is odd and leads to a triplet state.

Besides eqs 14 and 17 that invoke a modulator function either on or under the exponent, there is another way of writing the wave function:

$$\phi_{nl}(r) = r^l e^{-r^2/4} \sum_{k=0}^{\infty} h_k r^k \tag{22}$$

where we define a Taylor series $H(r) = \sum_{k=0}^{\infty} h_k r^k$. The SE for ϕ is then transformed into a second-order ODE for H similar to eq 19, so that h_k can be solved analogously. This is the typical textbook method for solving the hydrogen atom, where the asymptotic factors before H are determined by the analysis at $r \to 0$ and $r \to +\infty$, respectively. However, a crucial difference here is that $H(r)$, with an exact formula of $C\left(1 + \frac{r}{c}\right)^{\gamma} G\left(\frac{r}{r+c}\right)$ on $[0, \infty)$, does not yield a truncated series of r, in contrast to the hydrogenic radial wave function or any other well-known textbook example of exact analytic solutions. In fact, $H(r)$ here coincides with the biconfluent Heun function. The connection between this special function and the solution of harmonium problem was found in ref 16. It is worth noticing that the biconfluent Heun function can be defined for arbitrary energy and not limited to the eigenstate energy. For noneigenstate energies, $H(r)$ diverges faster than $e^{r^2/4}$ at $r \to \infty$ such that ϕ_{nl} as defined in eq 22 diverges at infinity and becomes a scattering state. For eigenstate energies, $H(r)$ still diverges but less quickly than $e^{r^2/4}$ such that ϕ_{nl} goes to zero at $r \to \infty$. In practical calculations, we are interested in the eigenstates only. With this biconfluent Heun function representation, we are faced with two challenges: (i) how to obtain the eigenstate energy; (ii) once given a highly accurate eigenstate energy, how to obtain a practically useful wave function by truncating the series of $H(r)$. For (i), a natural idea is to set $\phi_{nl}(r_0) = 0$ for a large enough r_0 upon truncating h_k to h_N. Again this leads to an algebraic equation of the energy that can be solved using Newton's method. However, we will show that even with an optimized r_0 the energy convergence with N is much slower than our new method invoking the modulator. But before that, let us begin with the second challenge, which reveals a major unexpected trouble associated with $H(r)$.

3. RESULTS AND DISCUSSION

To illustrate challenge (ii), in Figure 1 we compare the plot of $\phi_{00}^N(r)$, eq 22, using numerically exact h_k but truncated to h_N, with increasing N. As shown, for each given N, $\phi_{00}^N(r)$ has an artificial bump caused by the truncation. With increasing N, the bump moves away from the main peak of the wave function but grows larger. For $N = 100$, the artificial peak rockets to 10^8. Because of this reason, eq 22 is not a practically useful representation even though it is formally elegant without any parameter c. In comparison, our representation is numerically much more stable with a more transparent analytic structure particularly for asymptotic r. With increasing number of expansion coefficients, the wave function converges uniformly on $[0, \infty)$ to the true solution, for ground as well as all the excited states. This means that for arbitrary r, by keeping sufficiently large number of expansion coefficients, our formula can become arbitrarily accurate. Truncated to 20

https://doi.org/10.1021/acsomega.4c06679
ACS Omega 2024, 9, 46138−46147

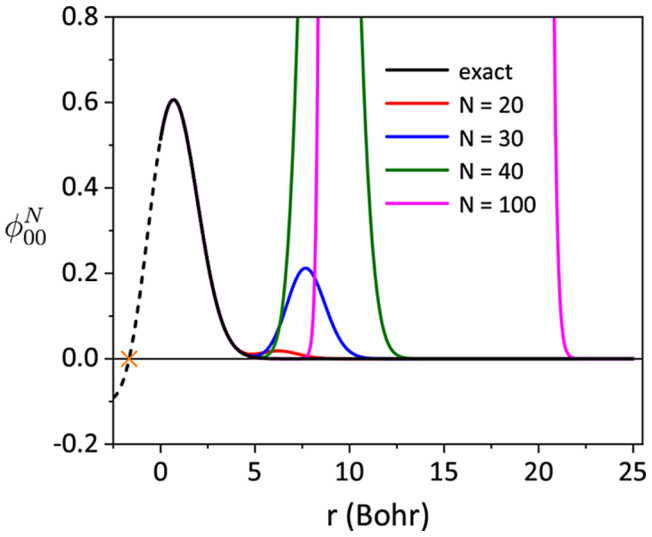

Figure 1. Series representation eq 22 for the ground state wave function truncated to the Nth order, denoted as ϕ_{00}^N, with $\lambda = 1$. For small r, $\phi_{00}^N(r)$ overlaps with the exact wave function calculated using eq 17 (black curve), however, it develops an artificial bump at a farther region that grows increasingly large for increasing N. We also extend the plot of the wave function to $r < 0$ using dashed lines, which intersect zero at a pseudo node marked by orange ×.

terms, the largest difference from the exact ground state curve is already less than 10^{-8}, which is not visible from the plot.

We also extend the plot of the wave function to $r < 0$ (dashed lines), which is beyond the physical domain. One can see that ϕ becomes zero at $r = r_0 \approx -1.6598$, which we refer to as a pseudo node and at which point our exponential assumption $\phi = Ce^{\beta}$ breaks down. However, this observation does not have conflict with the theorem that the ground state in 1D is nodeless in the defining domain. For higher excited states, there exist more pseudo nodes.

In our method, we have the freedom to choose parameter c. Empirically, we find that choosing c in a rather large positive interval can always yield reasonable results without harming the computational efficiency or robustness. As a default choice, we choose $c = c_\star$ such that $G(1) = G(0) = 1$ for ground state. This enables the variation of $G(z)$ to be small; for special λ such as $\lambda = \sqrt{2}$, $G(z)$ reduces to a constant. For excited state ϕ_{nl}, we choose $c_\star$ such that the nth derivatives of $G(z)$ at $z = 0$ and 1 become identical.

In Figure 2, we show the plot of $G(z)$ with $c_\star$ for ground state problems with different λ. As shown in Figure 2(a) and (b), G is a bounded and slowly varying function for $z \in [0, 1)$. For $0 \le \lambda \le \sqrt{2}$, the greatest variation of G is achieved at $\lambda \approx 0.7$, which is on the magnitude of 10^{-3} (see Figure 2b); for $\lambda > \sqrt{2}$, G becomes increasingly concave for larger λ but maintains a nearly quadratic shape. The corresponding $c_\star$ as a function of λ is shown in Figure 2c, where we have marked the special λ_i's using red triangles in the region $[0, 10]$ that have closed-form ground state solutions. The $c_\star$ for these special λ_i as well as other general λ's are not tremendously different; in fact $c_\star$ varies as a mild and smooth function of λ by only a few percentages. The specialness of λ_i is only manifested in $G(z)$ in the way that they truncate from infinite series into polynomials, yet in Figure 2a one can hardly notice any special feature from the line shape of these curves that distinguish themselves from other λ's.

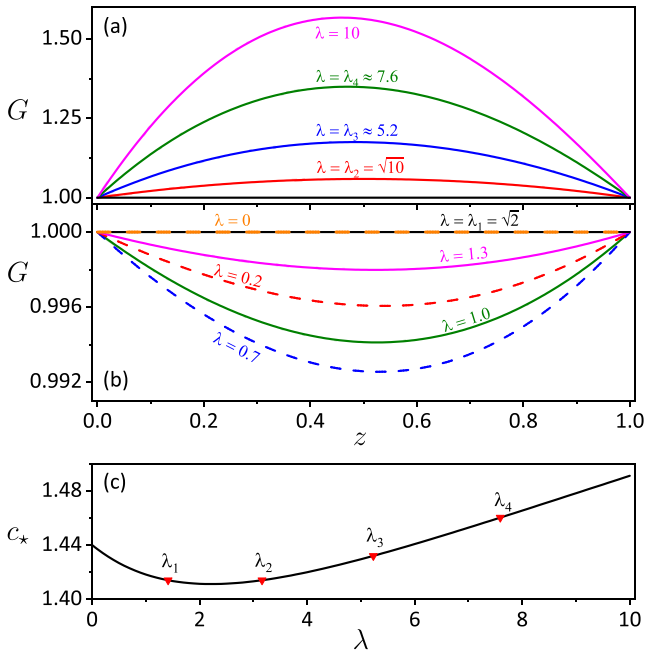

Figure 2. $G(z)$ calculated with $c_\star$ described in the text for the ground state problems for $\lambda \ge \sqrt{2}$ in (a) and $0 \le \lambda \le \sqrt{2}$ in (b). (c) $c_\star$ as a function of λ. The special λ_i's that have closed-form ground state solutions are marked by red triangles. In particular, $\lambda_1 = \sqrt{2}$, $\lambda_2 = \sqrt{10}$. Other λ_i's do not have simple elementary forms: $\lambda_3 \approx 5.2316$, $\lambda_4 \approx 7.5927$.

By introducing a modulator function, our method is much more efficient in representing the wave function than using the biconfluent Heun function (eq 22). This is shown in Figure 3 where we compare the energy convergence curve of the two methods for the ground state with $\lambda = 1$. In the biconfluent Heun function representation, the energy solution depends on r_0 where we set the truncated wave function to zero. As shown in the dot dash curves, for each finite r_0, the energy error saturates at a particular value. As $r_0 \to \infty$, the error tends to

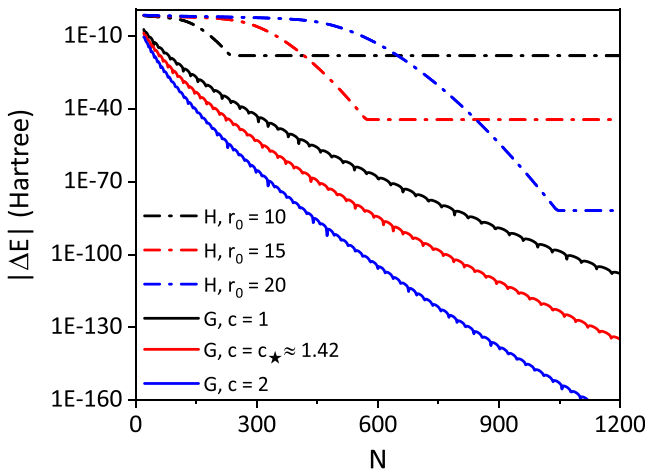

Figure 3. Ground state energy error as a function of the series truncation number N for our method with modulator G with different choices of c in comparison with the biconfluent Heun function method (labeled "H") with different choices of r_0 (in unit of Bohr). Here $\lambda = 1$. The periodically emerging spikes in our method are due to sign changes of the energy errors.

https://doi.org/10.1021/acsomega.4c06679
ACS Omega 2024, 9, 46138−46147

zero and the energy converges to the exact value. This is reasonable because the exact wave function becomes zero only at infinity; setting the wave function to be zero at larger r_0 shall bring the converged energy closer to the true value. However, achieving a more accurate energy is at the price of slow convergence at the beginning part of the curve. For example, for $r_0 = 10$, the energy drops to 10^{-10} at $N \approx 250$, while one needs $N \approx 400$ to achieve the same accuracy for $r_0 = 15$. This can be explained by the bump behavior in Figure 1: when the energy is accurate enough, the presence of the huge artificial bump due to the truncated series hinders us from imposing the condition $\phi_{00}(r_0) = 0$. For example, imposing this condition with $r_0 = 10$, one can expect to achieve reasonable energy solution using 250 terms in the truncated series, where the bump moves to the right side of this r_0; however, with these many terms one cannot achieve reasonable energy by imposing the condition at $r_0 = 15$, because this r_0 falls in the bump region of ϕ_{00}^N with $N = 250$.

By contrast, our method (eq 17) is free from such trouble. As shown by the solid lines, with reasonable choice of c (such as $c_\star$), our method converges faster than the best performance of the biconfluent Heun function method. This is guaranteed by design through the key step of fractional linear transformation $z = \frac{r}{r+c}$. By imposing the condition at $z = 1$ as in eq 11, we have essentially utilized the $r \to \infty$ condition in an indirect way, which is not achievable by any finite r_0 in the biconfluent Heun function method. As a side remark, although any c can fulfill our need and larger c appears to have faster convergence, it cannot be chosen too large. Otherwise, one will encounter similar behavior as the dot dash curves at the beginning part of the curve (not shown). As an additional remark, the energy convergence rates using modulator G (eq 17) and F (eq 14) are almost identical; with the same c, their curves essentially overlap each other.

Our method also greatly outperforms conventional basis expansion method, as illustrated in Figure 4a, where we compare the ground state energy convergence curve between the two methods. Here for the basis expansion method, we use as basis functions the radial eigen functions of a 3D isotropic harmonic oscillator with potential $\frac{1}{2}\alpha^2 r^2$ (α is a tunable parameter). Apparently, the numerical advantage of our method becomes even more pronounced than in Figure 3: the energy error drops to below 10^{-30} with 200 Taylor coefficients, while basis expansion method gives a much slower convergence even if one tries to optimize the basis, as shown by the performance with different α's. Such conclusions remain valid for excited states, as examplified by the excited state ϕ_{10} shown in Figure 4b, which is consistent with the observations in our previous work.[30]

The extremely accurate energies are largely due to the efficient representation of the wave function of our method. This is illustrated in Figure 5 where we compare the wave function residue defined by $\Delta\phi = (\hat{H} - E_r)\ \phi$ for the normalized ground state ϕ_{00} with $\lambda = 1$. By definition, $\Delta\ \phi$ is a function of r which measures how well ϕ satisfies the SE. As shown, choosing $c = 2$ and truncating the Taylor series to 10 terms, the maximum absolute residue is on the order of 10^{-7} for all $r \in [0, \infty)$, and this error drops to 10^{-14} when using $N = 30$ terms. Varying c can affect the size of the residue, but is of minor importance as our method performs way better than the basis expansion method which diverges as $r \to 0$. We note that this is because the wave function represented by the basis expansion using Gaussian functions fails to capture the cusp condition at $r = 0$, leading to a divergent residue once subtracting the Coulomb potential. Even if we neglect the

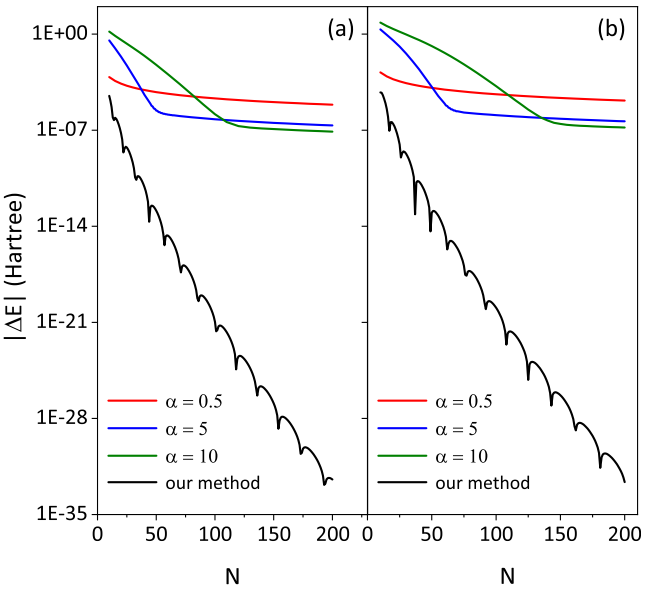

Figure 4. Energy error as a function of N for our method in comparison with the basis expansion method in the case of (a) ground state ϕ_{00} and (b) excited state ϕ_{10}. Here N is the number of terms used in G for our method and the number of radial eigen functions of a 3D isotropic harmonic oscillator that depends on parameter α used in the basis expansion method.

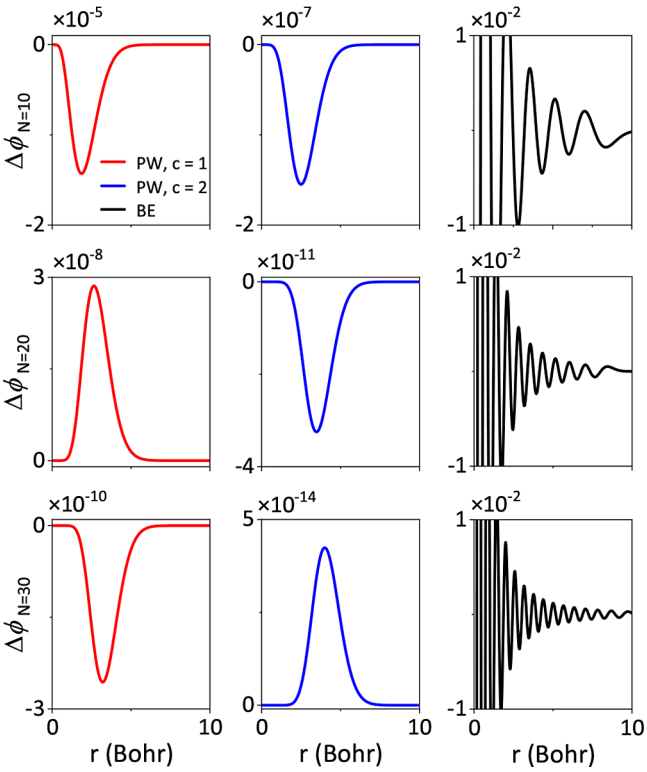

Figure 5. Residue of the ground state wave function, $\Delta\ \phi$, as a function of r of the present work (PW) in comparison with the basis expansion method (BE) with $\alpha = 0.5$. Here $\lambda = 1$ and subscript N denotes the truncation number or the number of basis functions. In the rightmost panel, the black lines obtained by BE diverge as $r \to 0$.

https://doi.org/10.1021/acsomega.4c06679
ACS Omega 2024, 9, 46138−46147

divergent region and focus on farther places, say $r \in [3, 10]$ Bohr, we see that basis expansion relies on increasingly rapid oscillations to bring down the maximum amplitude of the error, which can hardly drop below 10^{-4} with $N = 30$ and is far less efficient than our method. Importantly, the very simple residue pattern and the pointwise convergence behavior in our method is also a manifestation that it captures the most essential analytic structure of ϕ.

As λ grows large, the system becomes strongly correlated, as is manifested in Figure 6. In Figure 6a, we show the evolution

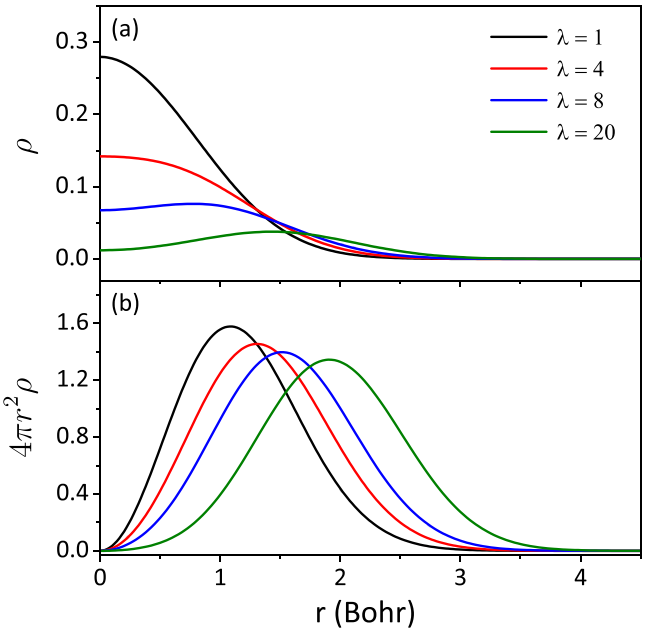

Figure 6. (a) Ground-state density ρ and (b) its radial distribution $4\pi r^2\rho$ as a function of r for increasing λ.

of the ground state density with λ. For small λ the density peaks at the origin, while for larger λ the peak flattens into a plateau and then develops a shoulder at a finite r. This is consistent with the plot of the radial density distribution in Figure 6b, which shows that the place with the largest probability of finding electrons keeps displacing to farther regions as λ grows, which is reasonable because the stronger Coulomb interaction tends to push the two electrons apart.

The most direct evidence of strong correlation comes from the natural occupation distributions and its evolution with increasing λ, as plotted in Figure 7. Because harmonium has spherical symmetry, the natural orbitals can be labeled in a way analogous to the hydrogenic atomic orbitals (*ns*, *np*, *nd*, *nf* and etc.) irrespective of the specific value of λ. We note that here one can have such orbitals as 1*p*, 1*d*, 1*f* and etc. attributable to the property of harmonic potential, which forms a distinction from the case of Coulomb potential where orbitals with high angular momentum can only arise for sufficiently large principle quantum numbers.

For the ground state as shown in Figure 7a, in the noninteracting case $\lambda = 0$, the 1*s* orbital is doubly occupied while the rest of the orbitals are unoccupied. As λ increases, contributions from other orbitals start to emerge. For example, although 1*s* orbital still dominates for small λ, the proportion of 3 1*p* orbitals quickly grows until they dominate over 1*s* orbital for $\lambda > 26$. Orbitals with higher angular momentum also have regions of dominance, which tend to occur at stronger

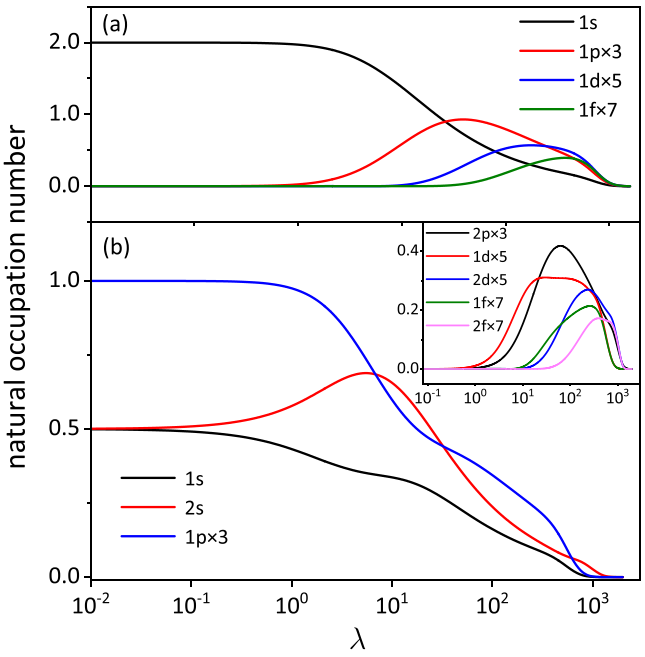

Figure 7. Evolution of the occupation number distribution over selected natural orbitals (multiplied by their respective degeneracy) with λ for (a) the ground state wave function and (b) the excited state $\chi_0(\boldsymbol{R})\psi_{10}(\boldsymbol{r})$. The horizontal axis is shown in logarithmic scale. Here we only show orbitals with significant occupations (>0.01) in the λ-region considered.

interaction. Interestingly, in the limit $\lambda \to \infty$, all natural orbitals tend to be equally occupied and no single natural orbital dominates over the others. Similar situations also occur in excited states, as exemplified by the low-lying excited state $\chi_0(\boldsymbol{R})\psi_{10}(\boldsymbol{r})$ in Figure 7b. Again, orbitals with high angular momentum emerge at large λ, although their evolution becomes more sophisticated; and occupation numbers tend to be uniformly distributed among different natural orbitals in the strong correlation limit. Our findings are consistent with the literature,[19,35−42] where extensive research has been conducted regarding the complex evolution of natural occupations of harmonium with λ, with particular emphasis on the limiting behavior as $\lambda \to 0$ and $\lambda \to \infty$. However, here we highlight the unusual situation at $\lambda \to \infty$ where infinitely many small occupations add up to a finite electron number (two), which differs from the commonly encountered strongly correlated chemical systems that are usually governed by only a few fractional occupations such as stretched N_2. Consequence of these special features of this toy model deserves further investigation, particularly for studying various approximation schemes in the case of this special type of strong correlation.

The harmonium problem is the simplest many-electron problem with the true two-body Coulomb interaction. For a general many-body problem, the standard way of solving for the wave function is through the configuration interaction (CI) method, i.e., representing the wave function through the expansion of determinants. It is well-known that the energy convergence with such expansions is slow. Here we use this simple exactly solvable problem to quantify its convergence rate. Our calculations were performed by modifying the PySCF code.[43−45] For the ease of code modification, here we fix $\lambda = 1$ and vary ω, for which the highly accurate energy can be converted from our exact solution for $\omega = 1$ through the

https://doi.org/10.1021/acsomega.4c06679
ACS Omega 2024, 9, 46138−46147

scaling relation. Besides, a modified version of the correlation consistent polarized n-tuple zeta (cc-pVnZ) basis set adapting to the harmonic one-body potentials was used. In particular, for each basis set, the number and symmetry of the basis functions remain unchanged from those conventionally used for the Coulombic helium atom, however, the parameters in the primitive Gaussians are reoptimized to capture the Gaussian decay of harmonic potentials instead of the exponential decay characteristic of the Coulomb potentials.

As shown in Table 1, the convergence with increasing number of determinants is indeed slow; with almost a million determinants the energy error only drops to 10^{-4}. The energy errors are approximately inversely proportional to the numbers of the basis function, which is consistent with the literature.[46] Moreover, the convergence rate does not seem to vary significantly with the interaction strength. By tuning ω from 0.5 to 1, the system becomes less strongly correlated, yet convergence is still slow. To bring the error down to 10^{-8}, one shall expect astronomical number of determinants.

Table 1. Error of the Ground-State Energy ΔE Calculated by the Full-CI Method with cc-pVnZ Basis[a]

basis	n	N	$\lvert\Delta E\rvert$ (ω = 1)	$\lvert\Delta E\rvert$ (ω = 0.5)
cc-pVDZ	5	45	5.5×10^{-3}	4.0×10^{-3}
cc-pVTZ	14	378	1.7×10^{-3}	1.2×10^{-3}
cc-pVQZ	30	1770	7.8×10^{-4}	5.6×10^{-4}
cc-pV5Z	55	5995	4.8×10^{-4}	2.9×10^{-4}
cc-pV6Z	91	16,471	3.8×10^{-4}	1.9×10^{-4}
cc-pV7Z[b]	140	39,060	2.2×10^{-4}	1.5×10^{-4}
cc-pV8Z[b]	204	83,028	2.0×10^{-4}	1.3×10^{-4}

[a]Here, n is the number of basis functions in each basis set and $N = n(2n-1)$ is the number of determinants involved. We fix $\lambda = 1$ and show the results for different ω. [b]The parameters in the primitive Gaussians are obtained through extrapolation from cc-pVnZ basis set with smaller n rather than a full optimization.

4. CONCLUSIONS

In this work, we extend our previously developed approach for finding the exact analytic form of stationary wave functions of one-electron Schrödinger equations to a two-electron harmonium problem with real-world two-electron Coulomb interaction of arbitrary strength λ. We show that the general solution for the ground state has a clear and unified analytic structure: a power pre-exponential factor, a Gaussian decay and a modulator function that be expressed as a Taylor series expansion of the interelectron distance r. This new representation refreshes our conventional thinking that the wave function has to be formulated as a summation in the Hilbert space, $\psi = \sum C_i\phi_i$. The modulator can be written either on or off the exponent. For particular choice of λ, the series function of the modulator is truncated to a polynomial, in line with the special solutions in the literature. Contrast between eq 21 and special solutions elucidates the general form of the solution that was previously unknown and conventionally regarded as too elusive to be accessible. For excited states, the analytic form involves additional factors accounting for the nodal information and spherical harmonic functions accounting for the angular information.

To the best of our knowledge, this is the first and simplest system with true two-electron Coulomb potential whose exact analytic structure of the wave function is completely deciphered. The relatively simple form particularly for the ground state gives us a hint of the analytic structure of a general two-electron and even many-electron system, and we believe it might not be as difficult as is generally believed. We admit that we have taken advantage of the harmonic one-body potential of this system such that we can separate variables, which is not achievable in the case of general one-body potentials. Nevertheless, we have recently found model two-electron systems for which one cannot achieve variable separation but we manage to write down the exact analytic solution. Amazingly, the resulting solution maintains the analytic structure that appeared again and again in our addressed problems, i.e., an exact factorized product of a pre-exponential power factor, and an exponential term with some leading decay and a modulator. This will be published in the near future.[47]

Our analytic solutions are not only formally exact, but also practically useful in computations. We have shown that our method has computational advantage over the biconfluent Heun function representation, and leads to much faster energy convergence than basis expansion methods in solving the SE after variable separation. For many-electron problems, this might suggest that there exists far more efficient ways of representing the wave function than the determinantal expansion as is performed by the CI method. This is reasonable because the CI wave function does not impose the correct asymptotic condition as in our formula, which greatly affects the efficiency of representation. Yet the validity and transferability of our proposition remains to be investigated, which we leave for future exploration.

As a final remark, we note that the harmonium problem has real-world Coulomb electron−electron interaction, from which we can gain insights into the development of density functional approximations. The critical universal functional defined by $F[\rho] = \min_{\Phi\to\rho}\langle\Phi|\hat{T} + \hat{V}_{ee}|\Phi\rangle$ and the exchange-correlation energy functional $E_{xc}[\rho]$ do not depend on the one-body potential, but critically depend on the two-body potential. Now with the exact wave function analytically accessible for any $\frac{\lambda}{r_{12}}$, we can study the exact constraints of E_{xc} particularly in the strong correlation limit. We have ongoing research along this line that will be published soon.[48]

■ ASSOCIATED CONTENT

Data Availability Statement

The data that support the findings of this study are available from the corresponding author upon reasonable request. We have submitted our Python code on Github with the following link: https://github.com/mangleywq/Harmonium

■ AUTHOR INFORMATION

Corresponding Author

Chen Li − *Beijing National Laboratory for Molecular Sciences, College of Chemistry and Molecular Engineering, Peking University, Beijing 100871, China;* orcid.org/0000-0003-2115-8694; Email: chenlichem@pku.edu.cn

Authors

Wenqing Yao − *Beijing National Laboratory for Molecular Sciences, College of Chemistry and Molecular Engineering, Peking University, Beijing 100871, China*

https://doi.org/10.1021/acsomega.4c06679
ACS Omega 2024, 9, 46138−46147

Zhiyuan Yin − *Beijing National Laboratory for Molecular Sciences, College of Chemistry and Molecular Engineering, Peking University, Beijing 100871, China*

Complete contact information is available at: https://pubs.acs.org/10.1021/acsomega.4c06679

Funding

The authors appreciate funding support from the National Key Research and Development Program of China (2023YFA1507000) and the National Science Foundation of China (8200906190).

Notes

The authors declare no competing financial interest.

■ ACKNOWLEDGMENTS

W.Y. acknowledges helpful discussion with Yunzhi Li and his code for calculating natural occupation numbers.

■ REFERENCES

(1) Hylleraas, E. A. Über den grundzustand des heliumatoms. *Z. Physik* **1928**, *48*, 469−494.
(2) Hylleraas, E. A. Energy Spectrum of the Excitations in Liquid Helium. *Z. Physik* **1929**, *54*, 347−366.
(3) Hylleraas, E. A.; Undheim, B. Numerische berechnung der 2 S-terme von ortho-und par-helium. *Z. Physik* **1930**, *65*, 759−772.
(4) Kinoshita, T. Ground state of the helium atom. *Phys. Rev.* **1957**, *105*, 1490.
(5) Klar, H. Exact asymptotic helium bound-state wavefunctions. *J. Phys. B: At. Mol. Opt. Phys.* **2001**, *34*, 2725.
(6) Drake, G. W. F.; Cassar, M. M.; Nistor, R. A. Ground-state energies for helium, H^-, and Ps^-. *Phys. Rev. A* **2002**, *65*, No. 054501.
(7) Li, J.; Holzmann, M.; Duchemin, I.; Blase, X.; Olevano, V. Helium Atom Excitations by the G W and Bethe-Salpeter Many-Body Formalism. *Phys. Rev. Lett.* **2017**, *118*, No. 163001.
(8) Kestner, N. R.; Sinanoğlu, O. Study of Electron Correlation in Helium-Like Systems Using an Exactly Soluble Model. *Phys. Rev.* **1962**, *128*, 2687−2692.
(9) Maksym, P. A.; Chakraborty, T. Quantum dots in a magnetic field: Role of electron-electron interactions. *Phys. Rev. Lett.* **1990**, *65*, 108−111.
(10) Merkt, U.; Huser, J.; Wagner, M. Energy spectra of two electrons in a harmonic quantum dot. *Phys. Rev. B* **1991**, *43*, 7320−7323.
(11) Jaskólski, W. Confined many-electron systems. *Phys. Rep.* **1996**, *271*, 1−66.
(12) Bielinska-Waz, D.; Karwowski, J.; Diercksen, G. H. F. Spectra of confined two-electron atoms. *J. Phys. B: At. Mol. Opt. Phys.* **2001**, *34*, 1987.
(13) Lamouche, G.; Fishman, G. Two interacting electrons in a three-dimensional parabolic quantum dot: a simple solution. *J. Phys.: Condens. Matter* **1998**, *10*, 7857.
(14) Kais, S.; Herschbach, D.; Levine, R. Dimensional scaling as a symmetry operation. *J. Chem. Phys.* **1989**, *91*, 7791−7796.
(15) Taut, M. Two electrons in an external oscillator potential: Particular analytic solutions of a Coulomb correlation problem. *Phys. Rev. A* **1993**, *48*, 3561−3566.
(16) Karwowski, J.; Witek, H. A. Biconfluent Heun equation in quantum chemistry: Harmonium and related systems. *Theor. Chem. Acc.* **2014**, *133*, 1494.
(17) White, R. J.; Brown, W. B. Perturbation Theory of the Hooke's Law Model for the Two-Electron Atom. *J. Chem. Phys.* **1970**, *53*, 3869−3879.
(18) Hall, R. W. Comparison of path integral and density functional techniques in a model two-electron system. *J. Phys. Chem.* **1989**, *93*, 5628−5632.
(19) Cioslowski, J.; Pernal, K. The ground state of harmonium. *J. Chem. Phys.* **2000**, *113*, 8434−8443.
(20) Matito, E.; Cioslowski, J.; Vyboishchikov, S. F. Properties of harmonium atoms from FCI calculations: Calibration and benchmarks for the ground state of the two-electron species. *Phys. Chem. Chem. Phys.* **2010**, *12*, 6712−6716.
(21) Rusin, T. M.; Zawadzki, W. Pauli exclusion operator: An example of Hooke's atom. *Phys. Rev. A* **2021**, *103*, No. 052221.
(22) Hou, L.; Irons, T. J. P.; Wang, Y.; Furness, J. W.; Wibowo-Teale, A. M.; Sun, J. Capturing the electron−electron cusp with the coupling-constant averaged exchange−correlation hole: A case study for Hooke's atoms. *J. Chem. Phys.* **2024**, *160*, No. 014103.
(23) Laufer, P. M.; Krieger, J. Test of density-functional approximations in an exactly soluble model. *Phys. Rev. A* **1986**, *33*, 1480.
(24) Kais, S.; Herschbach, D.; Handy, N.; Murray, C.; Laming, G. Density functionals and dimensional renormalization for an exactly solvable model. *J. Chem. Phys.* **1993**, *99*, 417−425.
(25) Taut, M.; Ernst, A. Two electrons in an external oscillator potential: multiplet splittings from exact solutions and one-particle approximations. *J. Phys. B: At. Mol. Opt. Phys.* **1998**, *31*, L35.
(26) Taut, M.; Ernst, A.; Eschrig, H. Two electrons in an external oscillator potential: exact solution versus one-particle approximations. *J. Phys. B: At. Mol. Opt. Phys.* **1998**, *31*, 2689.
(27) Coe, J. P.; Sudbery, A.; D'Amico, I. Erratum: Entanglement and density-functional theory: Testing approximations on Hooke's atom. *Phys. Rev. B* **2010**, *82*, No. 089902.
(28) Schubert, Y.; Marzari, N.; Linscott, E. Testing Koopmans spectral functionals on the analytically solvable Hooke's atom. *J. Chem. Phys.* **2023**, *158*, 144113.
(29) Li, C. Exact Analytical Solution of the Ground-State Hydrogenic Problem with Soft Coulomb Potential. *J. Phys. Chem. A* **2021**, *125*, 5146−5151.
(30) Tao, Y.; Li, Y.; Li, C. Is there a better way of representing stationary wave functions than basis expansion? *Int. J. Quantum Chem.* **2023**, *123*, No. e27083.
(31) Li, C. Exact analytical ground state solution of 1D H_2^+ with soft Coulomb potential. *J. Math. Chem.* **2022**, *60*, 184−194.
(32) Li, Y.; Li, C. Exact Analytical Form of Diatomic Molecular Orbitals. *ACS Omega* **2022**, *7*, 22594−22600.
(33) Arfken, G. B.; Weber, H. J.; Harris, F. E. In *Mathematical Methods for Physicists (Seventh ed.)*; Arfken, G. B.; Weber, H. J.; Harris, F. E., Eds.; Academic Press: Boston, 2013; pp 329−380.
(34) Feynman, R. P.; Cohen, M. Energy Spectrum of the Excitations in Liquid Helium. *Phys. Rev.* **1956**, *102*, 1189−1204.
(35) Cioslowski, J.; Buchowiecki, M. Collective natural orbital occupancies of harmonium. *J. Chem. Phys.* **2005**, *122*, 84102.
(36) Cioslowski, J.; Buchowiecki, M. Simple approximants for natural orbitals of harmonium. *J. Chem. Phys.* **2005**, *123*, 234102.
(37) Cioslowski, J.; Buchowiecki, M. Wigner molecules: Natural orbitals of strongly correlated two-electron harmonium. *J. Chem. Phys.* **2006**, *125*, No. 064105.
(38) Cioslowski, J.; Strasburger, K. Harmonium atoms at weak confinements: The formation of the Wigner molecules. *J. Chem. Phys.* **2017**, *146*, No. 044308.
(39) Cioslowski, J. Natural orbitals of the ground state of the two-electron harmonium atom. *Theor. Chem. Acc.* **2018**, *137*, 173.
(40) Cioslowski, J. Solitonic natural orbitals. *J. Chem. Phys.* **2018**, *148*, 134120.
(41) Giesbertz, K. J. H.; van Leeuwen, R. Natural occupation numbers: When do they vanish? *J. Chem. Phys.* **2013**, *139*, 104109.
(42) Giesbertz, K. J. H.; van Leeuwen, R. Long-range interactions and the sign of natural amplitudes in two-electron systems. *J. Chem. Phys.* **2013**, *139*, 104110.
(43) Sun, Q. Libcint: An efficient general integral library for g aussian basis functions. *J. Comput. Chem.* **2015**, *36*, 1664−1671.
(44) Sun, Q.; Berkelbach, T. C.; Blunt, N. S.; Booth, G. H.; Guo, S.; Li, Z.; Liu, J.; McClain, J. D.; Sayfutyarova, E. R.; Sharma, S.; Wouters, S.; Chan, G. K.-L. PySCF: the Python-based simulations of

chemistry framework. *Wiley Interdiscip. Rev.: Comput. Mol. Sci.* **2018**, *8*, No. e1340.
(45) Sun, Q.; Zhang, X.; Banerjee, S.; Bao, P.; Barbry, M.; Blunt, N. S.; Bogdanov, N. A.; Booth, G. H.; Chen, J.; Cui, Z.-H.; et al. Recent developments in the PySCF program package. *J. Chem. Phys.* **2020**, *153*, No. 024109.
(46) Cioslowski, J.; Strasburger, K. A Universal Power Law Governing the Accuracy of Wave Function-Based Electronic Structure Calculations. *J. Phys. Chem. Lett.* **2022**, *13*, 8055−8061.
(47) Yin, Z.; Deng, Y.; Wang, X.; Li, C. Exact analytic solution of the ground state many-body wave function, a case study of quartic potential problem, *in preparation*.
(48) Li, Y.; Li, C. Exact constraint of density functional approximations at the semi-classical limit, *in preparation*.

https://doi.org/10.1021/acsomega.4c06679
ACS Omega 2024, 9, 46138−46147